LA-UR-11-01310

Approved for public release; distribution is unlimited.

Title: Contour Method Advanced Applications: Hoop Stresses in Cylinders and Discontinuities

Author(s): Michael B. Prime (W-13)

Reference: Prime, M. B., 2011, "Contour Method Advanced Applications: Hoop Stresses in Cylinders and Discontinuities," Engineering Applications of Residual Stress, Vol. 8, T. Proulx, ed., Conf. Proc. of the Soc. for Exp. Mechanics Series, Springer New York, pp. 13-28. DOI: 10.1007/978-1-4614-0225-1_2

Contour Method Advanced Applications: Hoop Stresses in Cylinders and Discontinuities

Michael B. Prime (prime@lanl.gov)
Los Alamos National Laboratory, Los Alamos, NM 87545

ABSTRACT

The traditional contour method measures a cross-sectional map of residual stress by cutting a body carefully in two and measuring the surface contour. This talk will present two new advances, both motivated by the measurement of a single challenging part. The first advance is a two-step process for measuring hoop stresses in cylinders. In the first step, a cut is made to split the cylinder (from an "o" cross-section to a "c"). That cut releases a bending moment which would otherwise causes errors in the contour measurement. The amount the cylinder springs open or closed is measured and used to determine the bending moment stresses. In the second step, the traditional contour method is applied: a cut is made to measure the remaining hoop stresses on a cross section normal to the hoop direction. The total residual stresses are given by superimposing the bending stresses and the remaining stresses. In this paper, the two-step process is applied to measuring the stresses in a circumferential welded cylinder of depleted uranium and is compared to neutron diffraction results. The welded cylinder also contains a further measurement complication. The weld was only partial penetration, leaving part of the joint unwelded. The measured surface contour therefore had a discontinuity across the joint. Proper handling of the surface discontinuity is presented.

INTRODUCTION

The contour method is a relatively new method for measuring residual stress [1-3]. In the contour method, a part is carefully cut in two along a flat plane causing the residual stress normal to the cut plane to relax. The contour of each of the opposing surfaces created by the cut is then measured. The deviation of the surface contours from planarity is assumed to be caused by elastic relaxation of residual stresses and is therefore used to calculate the original residual stresses. One of the unique strengths of this method is that it provides a full cross-sectional map of the residual stress component normal to the cross section. The contour method is useful for studying various manufacturing processes such as laser peening [4-9], friction welding [5,10,6,11,12] and fusion welding [13-24].

The contour method has been extensively validated and applied for relatively simple geometries such as rectangular (or nearly rectangular) cross section bars and plates (examples above and [25-28]). Other applications involve more complicated cross sections but still prismatic extrusions [29,7,30] such as a railroad rails [31]. Occasionally, the contour method is applied to slightly more complicated geometries but ones that do not require much special effort [32-34].

This paper details a contour method application that involves two geometrical complications that require special attention. The first is the measurement of hoop stresses in a cylinder. The second is a discontinuity in the measured surface contour because of an unbonded butt joint.

Hoop Stresses in Cylinders

Pipes and cylinders are important geometries for residual stress measurement. A notable example is girth (circumferential) welds on piping and pressure vessels. Cracks cause concern for rupture in nuclear power plants [35,36]. To remain in service, such defected components must be demonstrated to be safe against rupture. Residual stresses are a main driver for the growth of cracks and must be known for crack growth and leak-before-break analyses [37-39]. Measurement of those stresses is difficult. Neutron diffraction is the most commonly published technique for measuring internal stresses. However, some components are too thick for neutron measurement and welds are often problematic because of spatial variations in the reference lattice constant caused by chemistry changes in and around the weld [40-42] or the presence of microstresses [42]. The deep hole method [43] has had the most success on very thick components but measures only a 1D stress profile. For all of the reasons, the ability of the contour method to measure a cross-sectional map of hoop stress in a cylinder is important.

Measuring hoop stresses in a cylindrical geometry requires special attention with the contour method. In simply-connected geometries, residual stresses must satisfy force and moment equilibrium over any cross section. Because the cylinder is a multiply-connected geometry, the residual hoop stresses can have a net bending moment through the thickness of a ring, see Fig. 1. Even for axisymmetric stresses, the moment is balanced by the opposite moment at any other cross section. For a contour method measurement of hoop stress, a radial cut is used. During cutting, because of the bending moment, excessive stresses build up at the cut tip and can cause plasticity. Since the contour method assumes elastic stress relaxation, errors can result and have been observed with the contour method [3] and similarly with the crack compliance method [44].

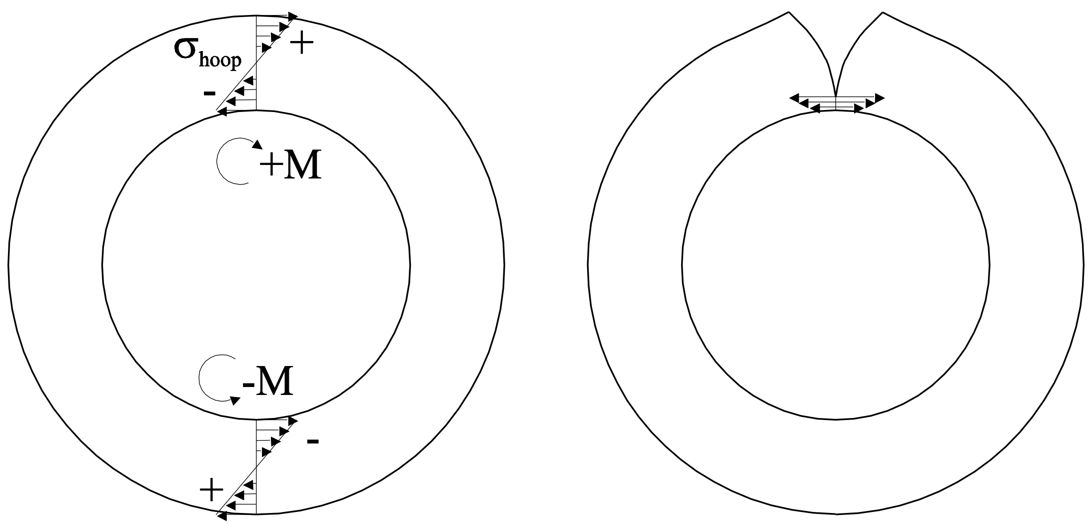

Fig. 1 Residual hoop stresses in cylinders can have a net bending moment (left), which can cause excessive stresses at the cut tip (right) when making a contour method measurement of hoop stress.

Discontinuity

Butt joints are often joined using only a partial penetration weld for several reasons. A partial penetration joint is often used for cost and simplicity reasons when the strength of a full penetration weld is not required. Other times, especially in pipes in cylinders, partial penetration is used to protect more delicate inner layers from heating or to maintain geometric tolerances inside the structure.

When a weld joint that includes an unfused portion is cut for a contour method stress measurement, the two sides of the unfused joints may deform such that there is a discontinuity in surface height on the cut surface. A conventional analysis of contour method data would involve smoothing and not allow a discontinuity. To achieve accurate results, the discontinuity must be properly preserved during data processing.

EXPERIMENTAL

Residual hoop stresses were measured in a cylinder with a partial-penetration weld butt-joint. The stresses measured with the contour method were recently compared with neutron diffraction measurements [45]. Space limitations in that paper prevented the presentation of details regarding the contour method measurements, which are detailed in this paper. The neutron measurement details are not repeated here.

Specimen

Fig. 2 shows a schematic, drawn approximately to scale, of the welded uranium sample studied in this work. The individual cylinders were as-cast depleted uranium. The sample had the form of a tube 131 mm in axial length with an inner diameter (ID) of 122 mm. At one end, termed the “A” end the outer diameter (OD) was 149 mm but at the opposite end, the ‘B” end, the outside surface was chamfered down to an OD of 137 mm, resulting in a wall thickness of 14 mm at the “A” end and 8 mm at the “B end. In this paper, the axial coordinate *y* is measured relative to the “A” end and the radial or *x* component is zero at the rotation axis.

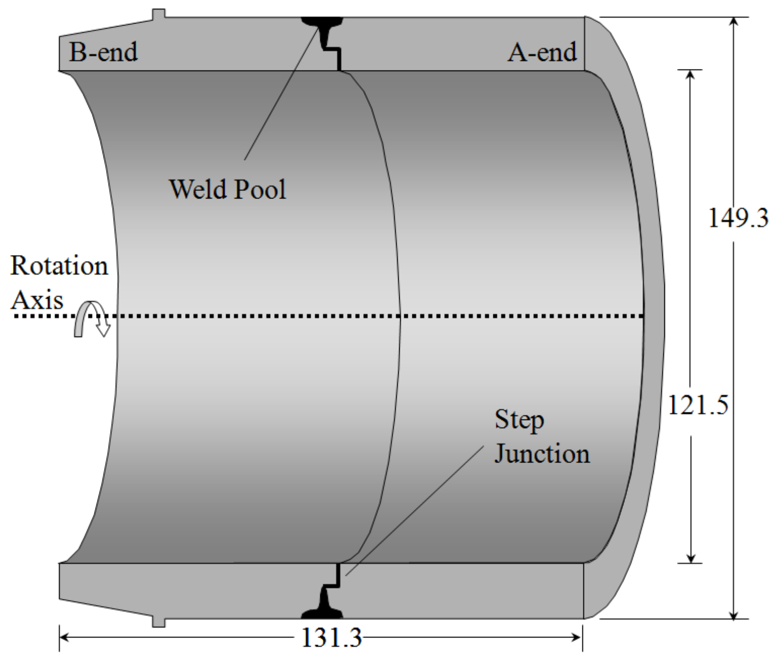

Fig. 2. Schematic of the electron beam welded uranium tube. Dimensions are approximately to scale. From [45].

The cast cylinders were machine fit at a step joint, as shown schematically in Fig. 2. The weld was a two-pass partial-penetration, autogenous electron beam weld centered at 64.8mm from the “A” end. The first pass, with the e- beam focused, penetrated roughly half of the thickness, bonding the two cast cylinders. The e- beam was then defocused for the second, cosmetic weld pass. The microstructure of the weld is detailed elsewhere [45].

Contour method procedure

In order to avoid plasticity at the cut tip, a novel, multiple-step variation of the contour method was used to measure hoop stresses over a radial-axial cross-section of the cylinder, see Fig. 3. The first cut severed the cylinder, which relaxed the bending moment. The resulting opening is measured and used to calculate the bending moment stresses. A subsequent cut is used to measure the remaining the remaining hoop stresses with the contour method. Because the bending moment is relaxed prior to the contour cut, plasticity issues are avoided.

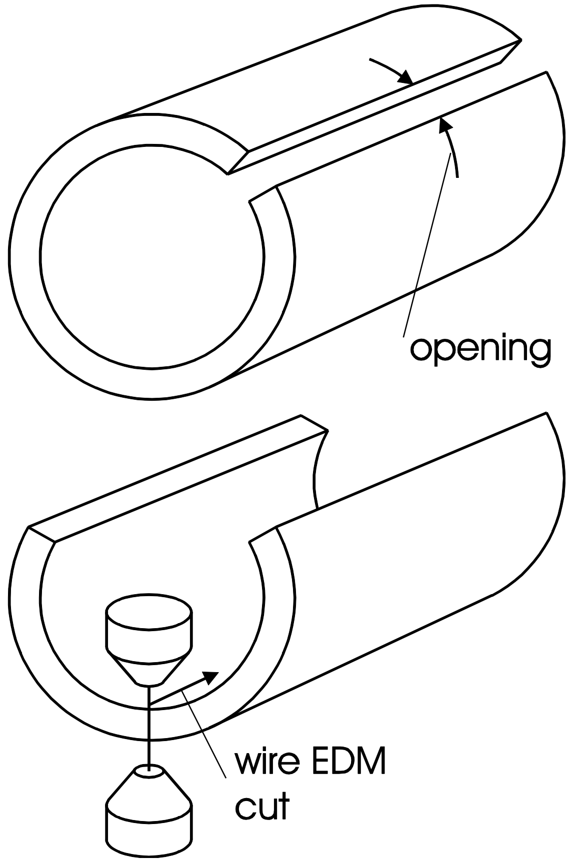

Fig. 3. Multi-cut process for measuring cylinders. The amount of opening, measured after the first cut, is used to determine the released bending moment prior to the final EDM cut used for the contour method. From [46].

A total of three EDM cuts were made on the uranium tube. Each cut operation used a 100 μm diameter brass wire and "skim cut" settings to reduce the introduction of new stresses [47]. Pairs of scribe lines, separated by about 6mm, were made along the length of the cylinder on the OD. The first EDM cut was made between the scribe lines with the wire oriented axially and translated radially. After unclamping, the relative displacements of the scribe lines were optically measured at 25 mm increments along the length of the tube. The second cut, taken at ~120° counter-clockwise from the first radial cut direction, was used to provide access for the third cut, but has no significant effect on the stresses measured by the third cut. The larger remaining section of the specimen was then measured with the contour method. A stainless steel fixture was machined to securely clamp the part along the ID and OD surfaces. To achieve better cut quality, the wire was now oriented in the radial direction and translated axially to make the cut.

After the final cut, the contours of the opposing surfaces were measured in a temperature controlled environment using a Coordinate Measuring Machine (CMM) with a 0.5 mm diameter ruby touch probe. The surfaces were scanned on a 0.5 mm grid giving about 6800 points per surface.

DATA

As a result of the first cut, the cylinder sprung open by 1.27 ± 0.01 mm uniformly along the length of the cut.

Fig. 4 shows the contours measured by the CMM on the two surfaces created by the third cut. One of the surfaces has been flipped to match the orientation of the other. The peak-to-valley range of the contours exceeds 40 μm. The close agreement between the two contours indicates that the part was clamped well during the cut and the experimental conditions were symmetric [48]. The contours are low in the weld region (right edge, mid height in this figure, see Fig. 2 for weld geometry) as would be expected if tensile stresses were relieved. A height discontinuity is evident cross the joint near the ID, which is mechanically admissible because of the un-joined material associated with the partial penetration weld.

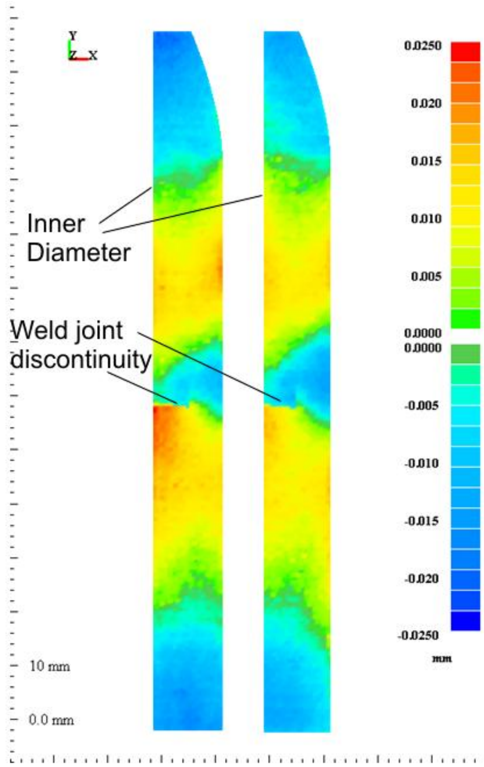

Fig. 4. Surface height contours measured on the two opposing surfaces created by the cut show the expected low region near the weld and also a discontinuity at the unwelded portion of the joint, near the ID.

ANALYSIS

The contour method analysis assumed isotropic elasticity with E=195 GPa, ν = 0.21.

A 3D elastic finite element (FE) model was used to calculate the stresses from the contour data. The perimeter of the cross-section was modeled based on the CMM data, and then the surface was meshed with 2D elements. The elements were not joined across the un-joined portion of the step joint. The 2D surface mesh was extruded circumferentially to produce 3D meshes 180 degrees and 120 degrees in extent to analyze the first and third cut data, respectively. The elements were approximately cubes 1.4 mm on a side near the cut surface and graded to be coarser in the circumferential direction farther away. The 180 degree mesh had almost 90,000 bi-quadratic (20 node) reduced integration hexahedral elements. No contact surfaces were used in the un-joined portion of the joint. Observation of the joint after cutting indicated that the gaps between the surfaces were sufficient to prevent contact.

First cut – bending moment

The first FE analysis, using the 180 degree mesh, was used to calculate the bending moment stresses released in the first cut. A symmetry plane was used to constrain one surface and concentrated forces were used to apply a bending moment on the opposite surface, see Fig. 5. The force magnitude was scaled until the surface in the half-symmetry model deformed the opposite amount of the opening observed experimentally.

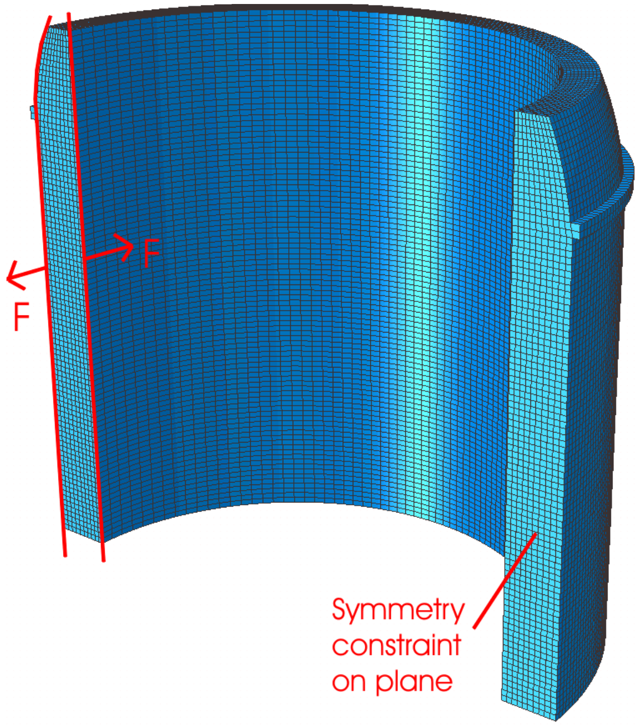

Fig. 5. Finite element calculation of bending moment stresses.

Contour method cut and discontinuity

In the contour method, the stresses are calculated in a finite element model by forcing the cut surface into the opposite shape of the measured contour [1]. For this experiment, converting the raw data into a form suitable for stress calculation generally followed standard procedure [3,2], except for some special care because of the discontinuity in the surface contours across the un-welded portion of the joint, see Fig. 4. The two opposing surfaces created by the cut were aligned with each other and then the data was interpolated onto a common grid and averaged. To handle the discontinuity, the surface was divided into two regions on either side of the weld joint with a few mm of overlap only in the part joined by the weld, see Fig. 6. Each region was then smoothed using quadratic bivariate spline fits with an optimal knot spacing determined to be about 5 mm. The two smooth surfaces were then joined together which resulted in discontinuities matching the data but a continuous joint in the weld region where the two regions overlapped.

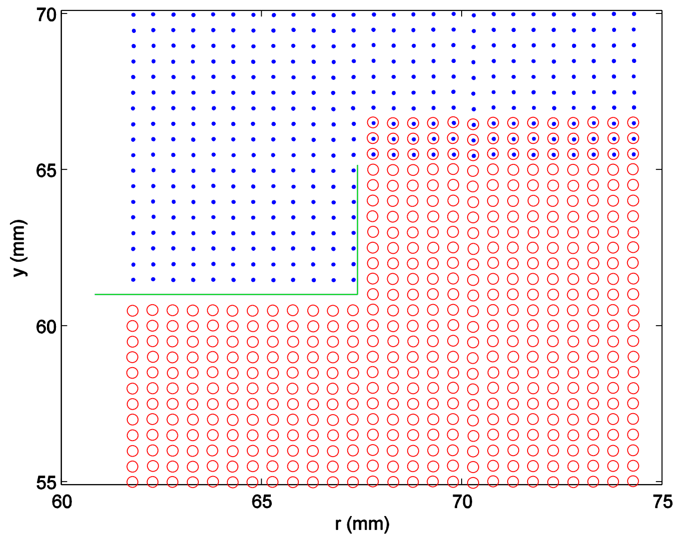

Fig. 6. Grid points used for fitting surface, zoomed in near weld region of Fig. 4. The green line indicates the unwelded portion of the joint and hence the discontinuity. The red and blue points are the grid points for the two fitting regions, which overlap in the weld region to ensure continuity.

The joined surface was evaluated at nodal coordinates in order to apply displacement boundary conditions to the FE model. Fig. 7 shows the FE model after the displacements were applied to the cut surface to calculate the stresses from the third cut. In this analysis, the other surfaces are unconstrained. The discontinuity across the joint is evident in Fig. 7. For the calculated stresses, a one standard deviation uncertainty of ± 25 MPa was estimated considering random errors in measured contours and uncertainty in the amount of data smoothing [2] but not any systematic errors.

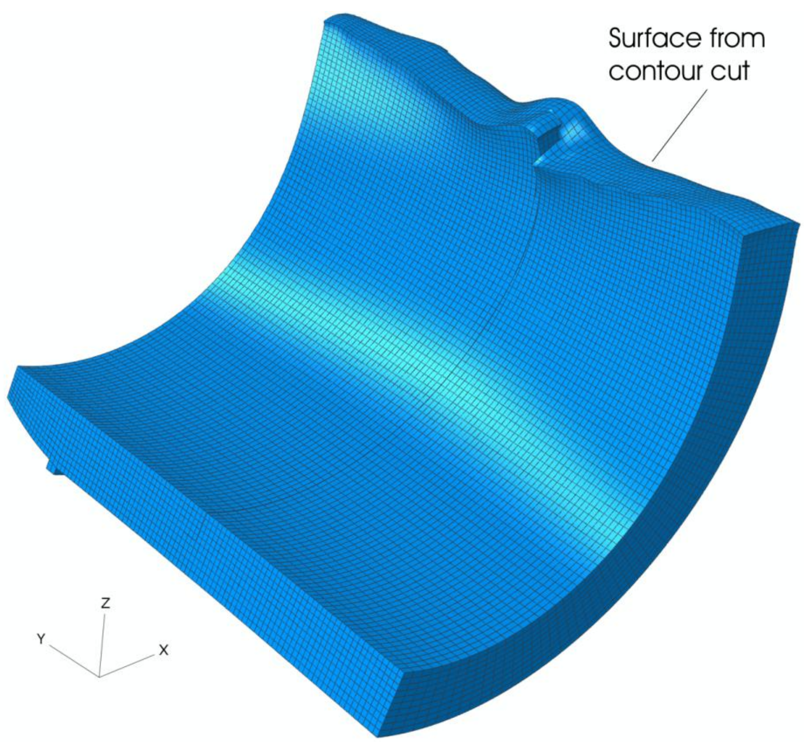

Fig. 7. The finite element model of a section of the cylinder with the cut surface deformed into the opposite of the measured contour. Displacements magnified by a factor of 300.

The stresses calculated from the contour analysis (Fig. 7) were added to the bending moment stresses calculated from the first cut (Fig. 5) to determine the total residual stress.

RESULTS

Bending moment stresses

The bending moment stresses given by the analysis of Fig. 5 are shown in Fig. 8. The stresses varied nearly linearly from about -60 MPa on the inner surface to about 50 MPa on the outer surface.

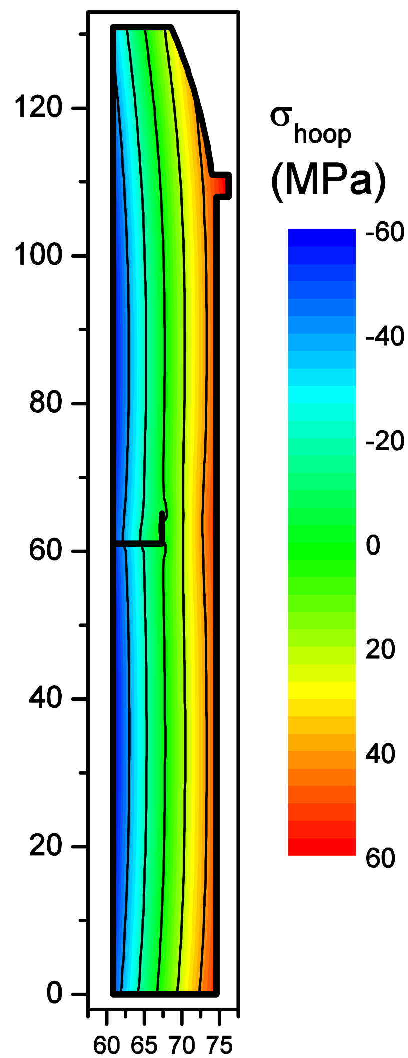

Fig. 8. Bending moment stresses calculated from the amount the cylinder sprung open (see Fig. 3) after the first cut.

In order to validate the bending moment stresses measured by the first cut, the results are compared with the neutron diffraction measurements [45]. The neutron diffraction measurements were taken before the cylinder was cut and, therefore, give the total stresses. Fig. 9 shows the comparison, with stresses plotted through the thickness of the cylinder. The neutron results are plotted for all of the measurement points, taken at multiple axial positions along the cylinder. The bending moment stresses measured by the first cut agree well with the linear trend in the neutron stresses, as they should. Since the non-bending stresses must satisfy equilibrium, an average of the total stress over the axial length of the cylinder should give only the bending stresses. In order to compare, such an average of the neutron stresses was calculated. Because the neutron sampling volumes were not equally spaced, the averaged was weighted in order to approximate a true spatial average. Also, the average was only taken at the three radial locations where the neutron measurements spanned the full length of the cylinder (the same data is potted later in Fig. 11, Fig. 12, and Fig. 13). The average of the neutron stresses is plotted in Fig. 9 and agrees quite well with the bending stresses measured by the first cut.

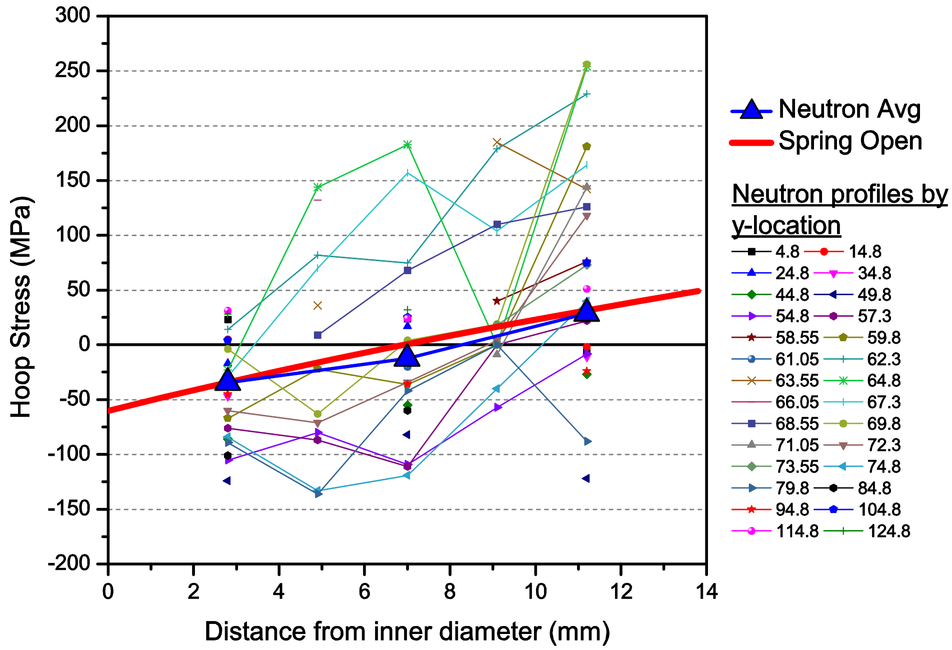

Fig. 9. Bending moment hoop stresses calculated from the “spring open” measured in the first cut compared with neutron diffraction measurements of *total stress*. The bending stresses agree well with the trend in the neutron data and with the average neutron stress.

Total stresses

Fig. 10 shows the hoop stresses measured in the welded cylinder. Fig. 10a shows the stresses calculated by the contour method analysis of Fig. 7. Fig. 10b shows the total stresses measured by the contour method, from adding the bending moment stresses of Fig. 8 to the stresses in Fig. 10a. Since the peak bending stresses are only about 15% of the peak total stress magnitudes, the correction is relatively minor. Fig. 10c shows the hoop stresses measured by neutron diffraction. The stress distribution is qualitatively similar, but the neutron-measured stresses are much lower in magnitude.

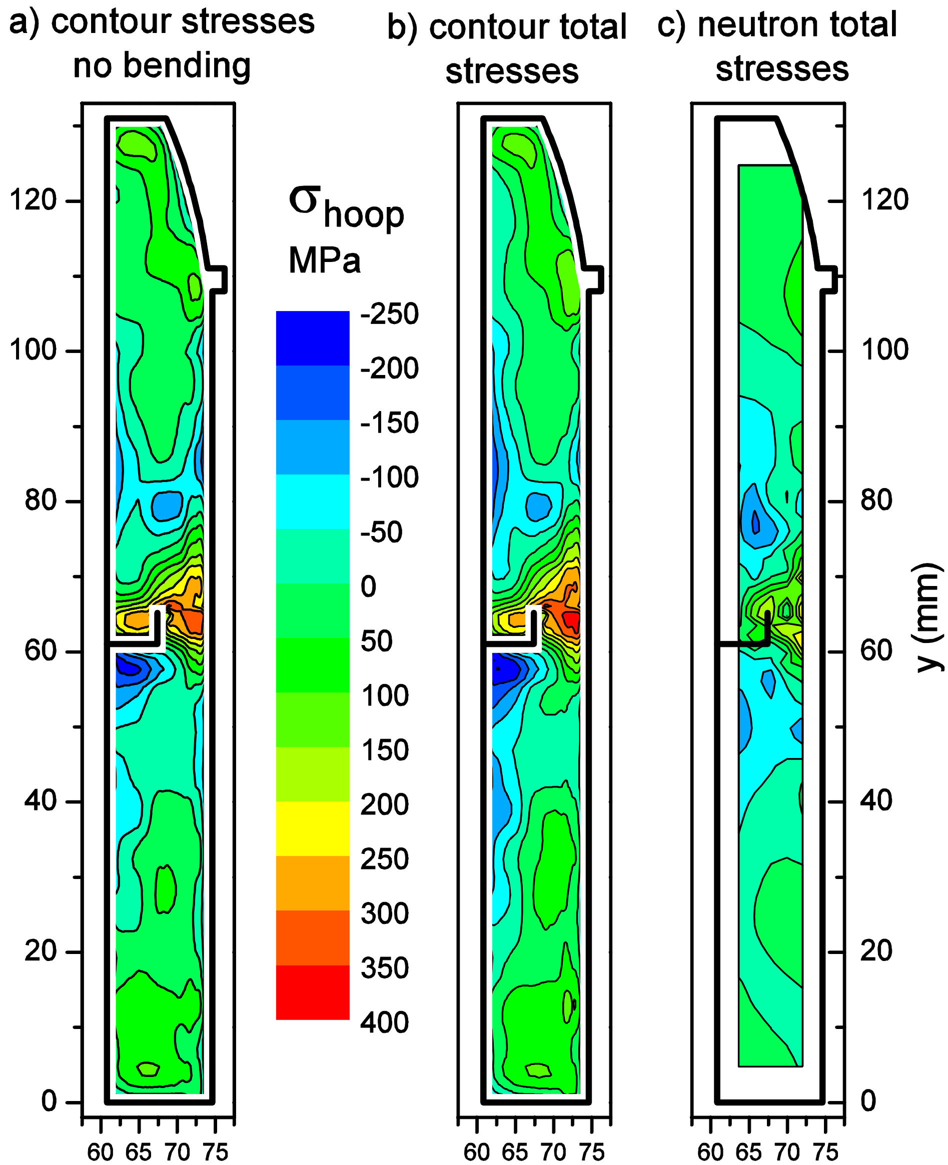

Fig. 10. Measured hoop stresses.

To further illustrate the issues, the results (Fig. 10 b and c) are compared along three neutron scan lines located at different locations through the thickness of the cylinder wall. Fig. 11 shows the comparison along the scan line near the cylinder inner diameter, which is the only scan line to cross the unfused portion of the joint. The contour and neutron results agree quite well away from the joint but not near the joint. Fig. 12 shows the comparison near the mid-thickness of the cylinder wall. Outside the weld region, results generally agree, with stresses differing nearly by a constant offset of ~40 MPa. One possible source for such an error can be the unstressed lattice spacing, also known as d_0, used in calculating strains and then stresses from the neutron diffraction measurements [41,42]. The weld stresses differ by more like 100 MPa. Fig. 13 shows the comparison along the scan line near the cylinder outer diameter. A shift of ~40 MPa would bring the comparison in better agreement away from the weld, but the contour stresses are again about 100 MPa higher in the high tensile stress region of the weld. For reference, note that the contour method FE stress calculation automatically enforces the constraint that the stresses satisfy force equilibrium. Because the neutron measurements do not cover the entire cross section, it is difficult to make conclusions about equilibrium.

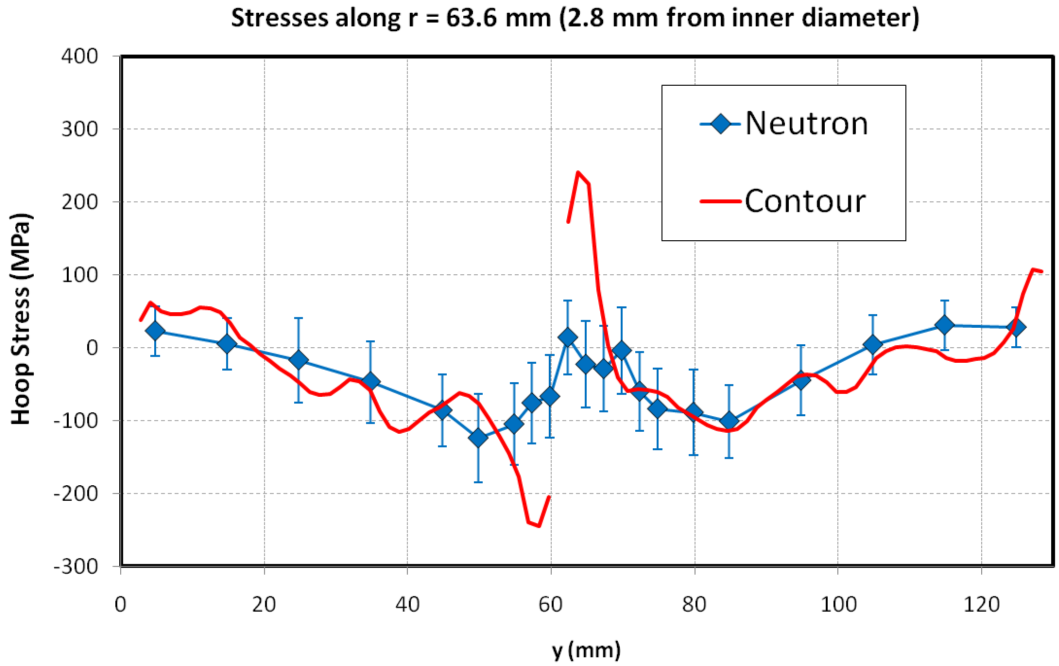

Fig. 11. Stresses along neutron scan line located about 2.8 mm from the cylinder inner diameter. This path crosses he unwelded joint at y=61

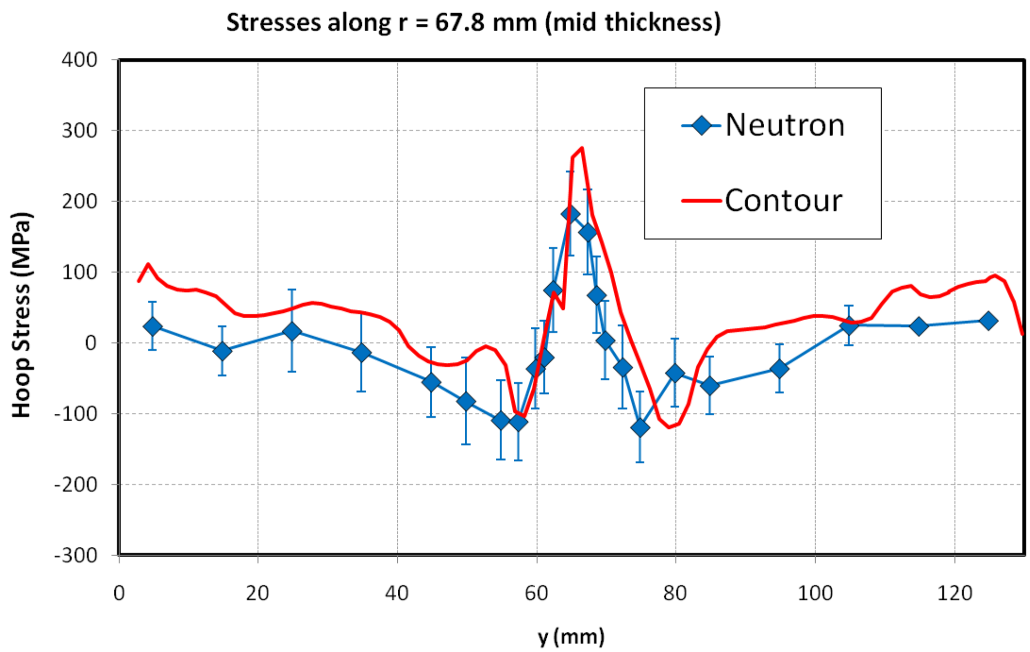

Fig. 12. Stresses along neutron scan line centered about mid-thickness in the cylinder.

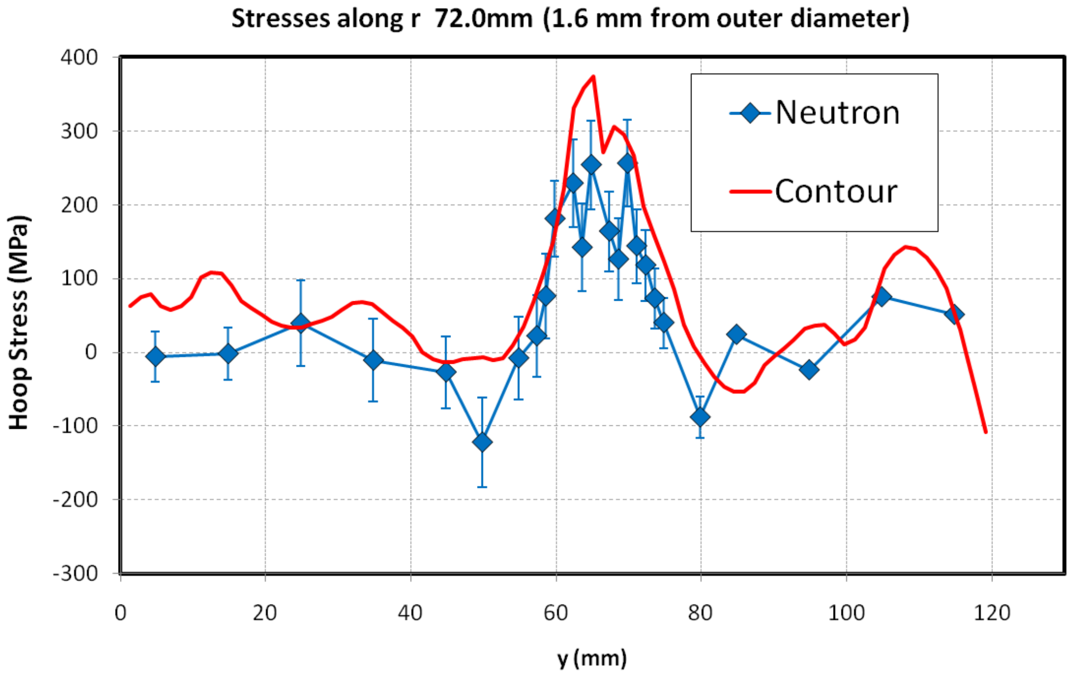

Fig. 13. Stresses along neutron scan line located about 1.6 mm from the cylinder outer diameter.

DISCUSSION

The contour method stresses are in reasonable agreement with the neutron results away from the weld region. The minor trend in the disagreement of the neutron stresses being lower by about 40 MPa might be explained by errors in the unstressed lattice spacing in the neutron measurements.

The contour method stresses are significantly higher than the neutron stresses in the tensile region of the weld. As will be discussed in the following paragraphs, there are many possible explanations for the difference. Some explanations are that the comparison does not fairly compare stresses at the same location. Other explanations include possible errors in both the neutron and contour measurements.

The neutron and contour measurements were not made over spatially identical regions. The neutron sampling volumes were 2×2×2 mm cubes. Because of issues with large grains, the neutron measurements were averaged around the circumference of the cylinder by rotating the cylinder during the measurements, effectively sweeping the sampling volume around the entire cylinder. There are two issues with the circumferential averaging. First, tolerances for both the part itself and the alignment and rotation during neutron measurements would make it likely that sharp discontinuities and gradients, such as in Fig. 11, would be smeared out in the neutron results. Second, the circumferential averaging would average in any changes near the start and stop of the weld, which can have significantly different stresses [22]. The contour results, by contrast, are taken only at the circumferential location of the cut. Unfortunately, the start-stop location of the weld was not known, so it is possible although unlikely that the contour results reflect localized stresses near the start or stop.

The results were challenging for neutron diffraction, which may have resulted in some errors. The uranium alloy has an orthorhombic crystal structure and had large grains, both of which made the neutron measurements more challenging and more prone to errors [45].

The two most common systematic errors associated with the contour method, plasticity and changing cut width, are unlikely to explain the difference in stress magnitudes measured by the two techniques. In tensile testing, the uranium showed yield strengths of about 200-250 MPa with strain hardening to over 400 MPa. The peak hoop stress in the cylinder exceeds the initial yield strength. (Because of the multi-axial nature of the stress and the strain hardening of the material, individual residual stress components exceeding nominal yield strength have been observed routinely in tensile stress regions near welds [49].) Because of the large measured stress magnitudes, plasticity at the tip of the cut could have caused errors. Plasticity effects are difficult to predict because they depend on prior history, strain hardening and cyclic plasticity. Nonetheless, simulations of plasticity effects for the contour method indicate possible errors in the position and shape of the stress profile, but not significant increases in peak stress magnitudes [50,51].

The contour method also assumes that the cut removes a constant width of material relative to the undeformed part. Because material ahead of the cut deforms as stresses are released, the cut width relative to the undeformed part evolves [48]. In the experiment reported in this paper, the cut width error was reduced by securely clamping the part during cutting, but could still cause errors of 5% to 10% in magnitude and spatial misalignment of results by a small amount. These effects do not likely explain the larger differences between the stresses measured with contour and neutron diffraction techniques.

The contour method has been validated in the literature many times by comparison with other measurement methods, primarily neutron and synchrotron diffraction. For specimens other than welds, the agreement between contour and other methods is generally very good [1,25,29,52,53,46,24]. "Very good" means that the measurements should agree to within one standard deviation error bars at 68% or more of the points. In welds, the agreement is less consistent. Often the agreement is good or very good [54,2,17,11,55,3,56,57]. Other times there are significant regions of disagreement [13,15,10,16,51,12]. There is a slight trend of the diffraction results having higher stresses than the contour results, in contrast with the results in this paper. However, the trend may not be significant. Because of chemistry changes, welds can be problematic for diffraction measurements [41,42]. Round robin studies with multiple diffraction measurements on the same sample often show a large amount of scatter in the results [58-60]. Therefore, one should not read too much into a comparison with neutron diffraction measurements from a single laboratory. There has been no comparable round robin with the contour method.

The contour and neutron results agree for the bending stresses but not the total stress. Is that possible physically and can the results then still validate the -cut process for the contour method? Yes. Equilibrium considerations dictate that the net bending moment be the same at any circumferential location around the cylinder[1]. Therefore, the circumferentially averaged hoop stress measured by neutrons must have the same moment as any local relaxation by a single cut. However, the distribution of circumferentially averaged stresses (neutron) certainly need not agree with a local measurement (contour).

CONCLUSION

In order to prevent or at least minimize plasticity errors, a multiple cut procedure has been developed for measuring hoop stresses in cylinders with the contour method. A first cut is used to sever the ring, allow it to open or close, and to determine the bending-moment portion of the residual stresses. For the welded cylinder in this study, the bending moment stresses agreed well with the stresses measured by neutron diffraction, validating this portion of the procedure. The bending moment stresses were a small fraction of the total stress magnitude, but could have a big effect on plasticity errors if they are not relieved.

A discontinuity was measured in the surface contour in the cut cylinder because of an unwelded portion of the joint. A procedure was developed to smooth the contour data but retain the discontinuity. High stress gradients were determined by the contour method in the discontinuity region.

Unfortunately, the total residual hoop stresses measured by the contour method did not agree with those measured by neutron diffraction, making for an unsatisfying validation of the overall procedure. However, because the neutron diffraction measurements were averaged over the circumference compared to the contour measurements taken at a single location, the differences may be real rather than an error in either measurement.

ACKNOWLEDGEMENTS

This work was performed at Los Alamos National Laboratory, operated by the Los Alamos National Security, LLC for the National Nuclear Security Administration of the U.S. Department of Energy under contract DE-AC52-06NA25396. By acceptance of this article, the publisher recognizes that the U.S. Government retains a

[1] Consider a free body diagram for any arbitrary segment of the cylinder.

REFERENCES

1. Prime MB (2001) Cross-sectional mapping of residual stresses by measuring the surface contour after a cut. Journal of Engineering Materials and Technology 123 (2):162-168
2. Prime MB, Sebring RJ, Edwards JM, Hughes DJ, Webster PJ (2004) Laser surface-contouring and spline data-smoothing for residual stress measurement. Experimental Mechanics 44 (2):176-184
3. Johnson G (2008) Residual stress measurements using the contour method. Ph.D. Dissertation, University of Manchester,
4. DeWald AT, Rankin JE, Hill MR, Lee MJ, Chen HL (2004) Assessment of Tensile Residual Stress Mitigation in Alloy 22 Welds Due to Laser Peening. Journal of Engineering Materials and Technology 126 (4):465-473
5. Hatamleh O, Lyons J, Forman R (2007) Laser peening and shot peening effects on fatigue life and surface roughness of friction stir welded 7075-T7351 aluminum. Fatigue and Fracture of Engineering Material and Structures 30 (2):115-130
6. Hatamleh O (2008) Effects of peening on mechanical properties in friction stir welded 2195 aluminum alloy joints. Materials Science and Engineering: A 492 (1-2):168-176
7. DeWald AT, Hill MR (2009) Eigenstrain based model for prediction of laser peening residual stresses in arbitrary 3D bodies. Part 2: model verification. Journal of Strain Analysis for Engineering Design 44 (1):13-27
8. Liu KK, Hill MR (2009) The effects of laser peening and shot peening on fretting fatigue in Ti-6Al-4V coupons. Tribology International 42 (9):1250-1262
9. Hatamleh O, DeWald A (2009) An investigation of the peening effects on the residual stresses in friction stir welded 2195 and 7075 aluminum alloy joints. Journal of Materials Processing Technology 209 (10):4822-4829
10. Woo W, Choo H, Prime MB, Feng Z, Clausen B (2008) Microstructure, texture and residual stress in a friction-stir-processed AZ31B magnesium alloy. Acta materialia 56 (8):1701-1711
11. Prime MB, Gnaupel-Herold T, Baumann JA, Lederich RJ, Bowden DM, Sebring RJ (2006) Residual stress measurements in a thick, dissimilar aluminum alloy friction stir weld. Acta Materialia 54 (15):4013-4021
12. Frankel P, Preuss M, Steuwer A, Withers PJ, Bray S (2009) Comparison of residual stresses in Ti6Al4V and Ti6Al2Sn4Zr2Mo linear friction welds. Materials Science and Technology 25:640-650. doi:10.1179/174328408x332825
13. Zhang Y, Pratihar S, Fitzpatrick ME, Edwards L (2005) Residual stress mapping in welds using the contour method. Materials Science Forum 490/491:294-299
14. Edwards L, Smith M, Turski M, Fitzpatrick M, Bouchard P (2008) Advances in residual stress modeling and measurement for the structural integrity assessment of welded thermal power plant. Advanced Materials Research 41-42:391-400
15. Kartal M, Turski M, Johnson G, Fitzpatrick ME, Gungor S, Withers PJ, Edwards L (2006) Residual stress measurements in single and multi-pass groove weld specimens using neutron diffraction and the contour method. Materials Science Forum 524-525:671-676
16. Withers PJ, Turski M, Edwards L, Bouchard PJ, Buttle DJ (2008) Recent advances in residual stress measurement. The International Journal of Pressure Vessels and Piping 85 (3):118-127
17. Zhang Y, Ganguly S, Edwards L, Fitzpatrick ME (2004) Cross-sectional mapping of residual stresses in a VPPA weld using the contour method. Acta Materialia 52 (17):5225-5232
18. Thibault D, Bocher P, Thomas M (2009) Residual stress and microstructure in welds of 13%Cr-4%Ni martensitic stainless steel. Journal of Materials Processing Technology 209 (4):2195-2202
19. Hacini L, Van Lê N, Bocher P (2009) Evaluation of Residual Stresses Induced by Robotized Hammer Peening by the Contour Method. Experimental Mechanics 49 (6):775-783
20. Turski M, Edwards L (2009) Residual stress measurement of a 316L stainless steel bead-on-plate specimen utilising the contour method. International Journal of Pressure Vessels and Piping 86 (1):126-131
21. Thibault D, Bocher P, Thomas M, Gharghouri M, Côté M (2010) Residual stress characterization in low transformation temperature 13%Cr-4%Ni stainless steel weld by neutron diffraction and the contour method. Materials Science and Engineering: A 527 (23):6205-6210. doi:DOI: 10.1016/j.msea.2010.06.035
22. Dai H, Francis JA, Withers PJ (2010) Prediction of residual stress distributions for single weld beads deposited on to SA508 steel including phase transformation effects. Materials Science and Technology 26:940-949. doi:10.1179/026708309x12459430509454

23. Simoneau R, Thibault D, Fihey J-L (2009) A comparison of residual stress in hammer-peened, multi-pass steel welds – A514 (S690Q) and S4150. Welding in the World 53 (5/6):R124-R134
24. Richter-Trummer V, Tavares SMO, Moreira P, de Figueiredo MAV, de Castro P (2008) Residual stress measurement using the contour and the sectioning methods in a MIG weld: Effects on the stress intensity factor. Ciência & Tecnologia dos Materiais 20 (1-2):114-119
25. Evans A, Johnson G, King A, Withers PJ (2007) Characterization of laser peening residual stresses in Al 7075 by synchrotron diffraction and the contour method. Journal of Neutron Research 15 (2):147-154
26. Martineau RL, Prime MB, Duffey T (2004) Penetration of HSLA-100 steel with tungsten carbide spheres at striking velocities between 0.8 and 2.5 km/s. International Journal of Impact Engineering 30 (5):505-520
27. Wilson GS, Grandt Jr AF, Bucci RJ, Schultz RW (2009) Exploiting bulk residual stresses to improve fatigue crack growth performance of structures. International Journal of Fatigue 31 (8-9):1286-1299
28. DeWald AT, Hill MR (2006) Multi-axial contour method for mapping residual stresses in continuously processed bodies. Experimental Mechanics 46 (4):473-490
29. DeWald AT, Hill MR (2009) Eigenstrain based model for prediction of laser peening residual stresses in arbitrary 3D bodies. Part 1: model description. Journal of Strain Analysis for Engineering Design 44 (1):1-11
30. Murugan N, Narayanan R (2009) Finite element simulation of residual stresses and their measurement by contour method. Materials & Design 30 (6):2067-2071. doi:10.1016/j.matdes.2008.08.041
31. Kelleher J, Prime MB, Buttle D, Mummery PM, Webster PJ, Shackleton J, Withers PJ (2003) The Measurement of Residual Stress in Railway Rails by Diffraction and Other Methods. Journal of Neutron Research 11 (4):187-193
32. Lillard RS, Kolman DG, Hill MA, Prime MB, Veirs DK, Worl LA, Zapp P (2008) Assessment of corrosion based failure in stainless steel containers used for the long-term storage of plutonium base salts. Corrosion 65 (3):175-186
33. Ismonov S, Daniewicz SR, Newman JJC, Hill MR, Urban MR (2009) Three Dimensional Finite Element Analysis of a Split-Sleeve Cold Expansion Process. Journal of Engineering Materials and Technology 131 (3):031007. doi:10.1115/1.3120392
34. Zhang Y, Fitzpatrick ME, Edwards L (2002) Measurement of the residual stresses around a cold expanded hole in an EN8 steel plate using the contour method. Materials Science Forum 404-407:527-532
35. Majumdar S (1999) Failure and leakage through circumferential cracks in steam generator tubing during accident conditions. International Journal of Pressure Vessels and Piping 76 (12):839-847
36. Wang X, Reinhardt W (2003) On the Assessment of Through-Wall Circumferential Cracks in Steam Generator Tubes With Tube Supports. Journal of Pressure Vessel Technology 125 (1):85-90
37. Bush SH (1992) Failure Mechanisms in Nuclear Power Plant Piping Systems. Journal of Pressure Vessel Technology 114 (4):389-395
38. Dong P, Brust FW (2000) Welding Residual Stresses and Effects on Fracture in Pressure Vessel and Piping Components: A Millennium Review and Beyond. Journal of Pressure Vessel Technology 122 (3):329-338
39. Bouchard PJ (2007) Validated residual stress profiles for fracture assessments of stainless steel pipe girth welds. International Journal of Pressure Vessels and Piping 84 (4):195-222
40. Withers PJ, Preuss M, Steuwer A, Pang JWL (2007) Methods for obtaining the strain-free lattice parameter when using diffraction to determine residual stress. Journal of Applied Crystallography 40 (5):891-904
41. Krawitz A (1994) Use of position-dependent stress-free standards for diffraction stress measurements. Materials Science and Engineering A 185 (1-2):123-130
42. Holden TM, Suzuki H, Carr DG, Ripley MI, Clausen B (2006) Stress measurements in welds: Problem areas. Materials Science and Engineering A 437:33-37
43. Smith DJ, Bouchard PJ, George D (2000) Measurement and prediction of residual stresses in thick-section steel welds. Journal of Strain Analysis for Engineering Design 35 (4):287-305
44. de Swardt RR (2003) Finite element simulation of crack compliance experiments to measure residual stresses in thick-walled cylinders. Journal of Pressure Vessel Technology 125 (3):305-308
45. Brown DW, Holden TM, Clausen B, Prime MB, Sisneros TA, Swenson H, Vaja J (2011) Critical Comparison of Two Independent Measurements of Residual Stress in an Electron-Beam Welded Uranium Cylinder: Neutron Diffraction and the Contour Method. Acta Materialia 59 (3):864-873. doi:10.1016/j.actamat.2010.09.022
46. Pagliaro P, Prime MB, Robinson JS, Clausen B, Swenson H, Steinzig M, Zuccarello B (2010) Measuring Inaccessible Residual Stresses Using Multiple Methods and Superposition. Experimental Mechanics. doi:10.1007/s11340-010-9424-5
47. Cheng W, Finnie I, Gremaud M, Prime MB (1994) Measurement of near-surface residual-stresses using electric-discharge wire machining. Journal of Engineering Materials and Technology-Transactions of the ASME 116 (1):1-7

48. Prime MB, Kastengren AL (2009) The Contour Method Cutting Assumption: Error Minimization and Correction. In: SEM Conference & Exposition on Experimental & Applied Mechanics, Indianapolis, IN USA, 2010. Society for Experimental Mechanics, Inc.,
49. Webster GA, Ezeilo AN (2001) Residual stress distributions and their influence on fatigue lifetimes. International Journal of Fatigue 23 (SUPPL. 1):S375-S383
50. Shin SH (2005) FEM analysis of plasticity-induced error on measurement of welding residual stress by the contour method. Journal of Mechanical Science and Technology 19 (10):1885-1890
51. Dennis RJ, Bray, D.P., Leggatt, N.A., Turski, M. Assessment of the influence of plasticity and constraint on measured residual stresses using the contour method. In: 2008 ASME Pressure Vessels and Piping Division Conference, Chicago, IL, USA, 2008. ASME, pp PVP2008-61490
52. Pagliaro P, Prime MB, Clausen B, Lovato ML, Zuccarello B (2009) Known Residual Stress Specimens Using Opposed Indentation. Journal of Engineering Materials and Technology 131:031002
53. Pagliaro P, Prime MB, Swenson H, Zuccarello B (2010) Measuring Multiple Residual-Stress Components Using the Contour Method and Multiple Cuts. Experimental Mechanics 50 (2):187-194. doi:10.1007/s11340-009-9280-3
54. Zhang Y, Ganguly S, Stelmukh V, Fitzpatrick ME, Edwards L (2003) Validation of the Contour Method of Residual Stress Measurement in a MIG 2024 Weld by Neutron and Synchrotron X-ray Diffraction. Journal of Neutron Research 11 (4):181-185
55. Kartal ME, Liljedahl CDM, Gungor S, Edwards L, Fitzpatrick ME (2008) Determination of the profile of the complete residual stress tensor in a VPPA weld using the multi-axial contour method. Acta Materialia 56 (16):4417-4428
56. Smith MC, Smith AC (2009) NeT bead-on-plate round robin: Comparison of residual stress predictions and measurements. International Journal of Pressure Vessels and Piping 86 (1):79-95
57. Bouchard PJ (2009) The NeT bead-on-plate benchmark for weld residual stress simulation. International Journal of Pressure Vessels and Piping 86 (1):31-42. doi:DOI: 10.1016/j.ijpvp.2008.11.019
58. Wimpory RC, Ohms C, Hofmann M, Schneider R, Youtsos AG (2009) Statistical analysis of residual stress determinations using neutron diffraction. International Journal of Pressure Vessels and Piping 86 (1):48-62. doi:DOI: 10.1016/j.ijpvp.2008.11.003
59. Withers PJ, Webster PJ (2001) Neutron and Synchrotron X-ray Strain Scanning. Strain 37 (1):19-33. doi:10.1111/j.1475-1305.2001.tb01216.x
60. Hughes DJ, Webster PJ, Mills G (2002) Ferritic steel welds - A neutron diffraction standard. Materials Science Forum 404-407:561-566